

EXTRACTION OF ROAD MARKINGS FROM MLS DATA: A REVIEW

E. Barçon^{1*}, T. Landes², P. Grussenmeyer², G. Berson¹

¹Innovation department, TT Géomètres-Experts, 75011 Paris, France - (e.barcon, g.berson)@ttge.fr

²Université de Strasbourg, CNRS, INSA Strasbourg, ICube Laboratory UMR 7357,

Photogrammetry and Geomatics Group, 67000, France (tania.landes, pierre.grussenmeyer)@insa-strasbourg.fr)

Commission II

KEY WORDS: Mobile Laser Scanning, Vectorization, Point Clouds, Automation, Road Markings

ABSTRACT:

Nowadays, Mobile Laser Scanning (MLS) systems are more and more used to realize extended topographic surveys of roads. Most of them provide for each measured point an attribute corresponding to a return signal strength, so called intensity value. This value enables to easily understand uncolored MLS as it helps to differentiate materials based on their albedo. In a road context, this intensity information allows to distinguish, among others, the main subject of this paper, i.e. road markings. However, this task is challenging. Road marking detection from dense MLS point cloud is widely studied by the research community. It might concern road management and diagnosis, intelligent traffic systems, high-definition maps, location and navigation services. Dense MLS point clouds provided by surveyors are not processed online, they are thus not directly applicable to autonomous driving, but those dense and precise data can be for instance used for the generation of HD reference maps. This paper presents a review of the different processing chains published in the literature. It underlines their contributions and highlights their potential limitations. Finally, a discussion and some suggestions of improvement are given.

1. INTRODUCTION

Mobile Laser Scanning (MLS) is now a very popular technique to obtain, on large areas, dense points clouds associated with panoramic images. This technique can be used to conduct surveys of roadways for transportation agencies, local authority, or highway operators. The data collected during the survey can be used for a wide range of applications, like diagnostics or evaluations for maintenance, land-use planning, or to elaborate a topographic map.

In this paper, we focus on the detection and extraction of road markings from dense MLS point clouds with intensity information. Road markings are essential elements that must appear on a topographic map, especially in an urban context. This paper is a review of the different techniques proposed in the literature. It underlines the solutions with highest potential and highlights also their limitations.

The first section presents a review of the state of the art. The second resumes the weaknesses of the presented techniques and finally the last section presents some perspectives.

2. STATE OF THE ART

The structure of this chapter follows the common chronological processing chain. Most of the time, it includes a pre-processing step (2.1) of the raw point clouds and a ground segmentation (2.2). Then the detection of the marking from the ground points

(2.3), is followed by a refinement of the results (2.4). Next, a classification of the resulting markings is performed (2.5) before a final vectorization and the export of the results (2.7). Some Deep-Learning approach are presented apart from the others in the section (2.6). Finally, a summary table is presented at the end of the paper (Table 1).

2.1 Pre-processing

Unlike images, point clouds are unstructured data i.e. no spatial relationship between two points of the cloud can be assumed without any prior calculations.

Detection of road markings belongs generally to a larger processing chain leading to road modeling. For computational purpose, massive MLS point clouds are segmented in blocks of small areas. This decomposition is not without consequences, since the spatial continuity of the scanned surfaces is broken. To overcome this problem, a certain overlap between the blocks is kept. Mi et al. (2021) propose an overlap distance corresponding to the longest expected marking. Another drawback of this necessary decomposition is that the results of the different blocks must be merged afterwards.

To reduce the data volume from the start, Soilán et al. (2017) remove all points farther than 10 m from the sensor, considering they are irrelevant. On top of that, and in the more general case,

* Corresponding author

a preliminary ground/non-ground segmentation is almost always performed.

2.2 Ground/ non-ground segmentation

The first segmentation step aims to separate ground from non-ground. This step is very important, because it enables to optimize the further treatments by focusing the search on the road and getting rid of unwanted objects such as cars, cyclists, pedestrians, and other moving objects.

Different methods are presented for extracting the ground in a road context. Yao et al. (2018) suggest the use of the scan-line structure. Supposing that the MMS device collects points in the way of single line profiles, the point cloud can be decomposed using it. A scan-line is simply a set of points that are almost aligned along a straight line because they were acquired during the same spin of the lidar head. On each scan-line, the authors detect the curb (or road boundary) by identifying abrupt changes of slope or elevation.

However, this approach is not always suitable, depending on the kind of sensors used (multi-head devices) or the number of passes on the same street. The general idea is to study the road using cross-sections i.e. perpendicularly to the road direction. This requires the prior orientation of the point clouds along the chosen axis or at least the knowledge of the street orientation. By exploiting these cross-sections, the authors try to put the data in a kind of “canonical” form, knowing that they will correspond to a typical profile. Yu et al. (2015) proposed to detect the curbs by thresholding the slope and altitude along successive profiles. Yang et al. (2020) exploit a pseudo scan-line structure to detect the curb positions using a sliding window. In a previous work, we used a sigmoid adjustment to detect and vectorize curbs Barçon et al. (2022). In these articles, the road area is deduced from the curb detection results.

By using the final adjusted trajectory of the sensor during the acquisition as well as some calibration information, Guo et al., (2015) and Yang et al. (2020) deduced the road’s altitude. Using this information, Guo et al. (2015) select road’s points as those verifying a cartesian plane equation.

Assuming that the road direction is aligned with the x axis, Jung et al. (2019) used the robust RANSAC algorithm to fit the y, z coordinates with a second order polynomial. The polynomial is constrained with a negative first major coefficient. This method is more robust than using a plane equation because most of the time a cambered cross-section is observed.

Outside this structuring in profiles, some global approaches have been proposed.

Kumar et al. (2013) use snake curve technique. This image-based approach is based on a mixture of elevation, reflectance and pulse width information gathered by the LiDAR sensor. The external (boundary attraction) energy is then deduced from it, the internal energy model (elasticity and stiffness) is also defined before the snake adjustment initialization based on the trajectory.

Cheng et al. (2017) and Ye et al. (2020) use an upward growing region using voxels with local and global height thresholds. Slices of the road are subdivided into voxels. For each 2D location, the clustering process progresses from bottom to top. If

the top voxel exceeds a threshold, the area is labelled as non-ground.

After this voxel upward growing region, Cheng et al. (2017), refine the segmentation by generating a Digital Terrain Model (DTM) using Inverse Distance Weighted (IDW) interpolation. A high-pass filter is used to estimate the roughness of the surfaces on the DTM. By thresholding the roughness map, the final road area corresponds to the largest smooth surface.

Fang et al. (2022) extract the ground using the Cloth Simulation Filter (CSF) (W. Zhang et al., 2016) method after partitioning the point clouds into smaller blocks.

Wen et al. (2019) used the boundary extraction method presented by (Zai et al., 2018). This method is based on supervoxel generation followed by a graph cut algorithm that select the road boundary among the supervoxels’s facets.

This section enumerated some techniques used for ground segmentation. Some of them are sensor dependent, or depend on the availability of the trajectory, on points attributes. Also, the choice of a technique and its parameters depends on the tolerance regarding the vertical object starters remaining in the ground class. In lot of works, the ground segmentation is more like a segmentation of the roadway. By doing so, the markings of cycling path or others on the sidewalk are deleted at this moment.

After this step, the segmented point cloud is very often converted in an image, i.e. the points are projected on a plane. The image approach is more comfortable especially because the available tools are more numerous than for 3D point clouds processing. After this step, the data are conditioned for the extraction of the road markings

2.3 Road marking detection

All methods proposed in the literature exploit the high radiometric contrast between the markings and the road asphalt. Road markings are emphasized by high intensity value returned by the laser beam.

Different thresholding techniques have been presented. Because the laser pulse intensity decreases with the range and also depends on the incidence angle, many authors propose empirical adaptative thresholds based on these two attributes.

Jaakkola et al. (2008) reduce the variance of the measured intensity along a transversal profile of the road. Assuming that the median intensity along a transversal profile of the road can be mostly described by a second-degree curve, the authors use it to model and then rectify the measured values.

In a very similar way, Zhang et al, (2016) notice the affine relation between the intensity and the cosine of the scan-angle of each point. Using this relation, the authors “normalize” the intensity values. Wan et al. (2019) correct the intensity using a 3rd degree polynomial based on the range distance. Then an iterative maximum entropy threshold is used to extract the markings.

These three first approaches rectified individually each point, using a correction model. However, the scan angle and range attributes for each point are not always available. Others approaches, less fine since they don’t rectify each point

individually, have been proposed in order to do a locally effective threshold.

(Yang et al., 2020), examine the intensity value along a scan-line profile and threshold the intensity value and intensity gradient. The left and right edges of each marking is thus detected. The confrontation of successive profiles' results allows to delete noisy detections.

Kumar et al. (2014) subdivide the orthophoto into rectangular blocks having a similar range (scanner to surface distance). The different thresholds are lower as the block is far from the sensor trajectory and based on a reference empirical value.

Yu et al. (2015) proposed a similar approach using the range (Figure 1) and Soilán et al. (2017) used the scan-angle. For both, each subpartition is thresholded independently using the Otsu method (Otsu, 1979). This method supposed the image is bimodal. The threshold is determined by minimizing the intra-class variance, which is equivalent to maximizing inter-class variance.

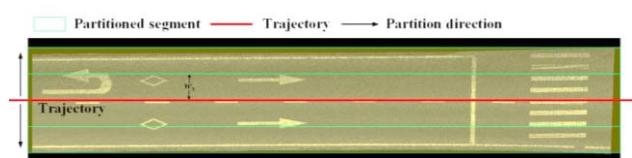


Figure 1. Multisegment partition suggested by (Yu et al., 2015).

Other authors proposed different adaptative thresholding methods that can be applied without the range and incidence angle information. Yao et al. (2018) use the Bradley and Roth (2007) technique. Their technique allows to quickly compare each pixel value with the mean of its neighbourhood pixels and then threshold the difference.

Fang et al. (2022) use the technique presented by Guan et al. (2014) consisting in decomposing the road area depending on the point density. The assumption is that the distance sensor to object is inversely proportional to the point density. Using a point density histogram along a cross-section, the densest area is considered as a starting position and the standard deviation can be estimated. From this starting position, subareas are created on each side, with a width corresponding to the previously estimated standard deviation. Each area is then independently thresholded using the Otsu method.

Ye et al. (2020) used a simple threshold method for specific markings like arrows, texts and symbols. For the linear shaped markings, the distance to the preliminary detected road edges is also thresholded to introduce *a priori* knowledge and reduce false positives.

Pan et al. (2019) preferred the maximum entropy technique to define the optimal intensity threshold.

All these techniques are more or less robust towards the inhomogeneous intensity values of the point clouds. In addition to the range and incidence angle influence, the changing weather and illumination conditions (difference of materials' albedo, shadows, etc) also cause intensity variations. Local thresholding methods are more resilient to these disturbing elements.

Despite the use of robust thresholding techniques, the results still contain noise. Moreover, the road markings may have rough or damaged shapes. That's why some filtering and improvement must be performed before a proper classification.

2.4 Shape improvement and clustering

As a result of the thresholding, a binary image is obtained. However, this image contains noise that must be reduced. Inliers must also be gathered to form markings candidates.

The raw binary image can be refined using Statistical Outlier Removal (SOR) as presented by Ye et al. (2020). The assumption made is that the noise is sparser than inliers.

Cheng et al. (2017) apply a median filter and a minimum area threshold for Connected Components (CC) to filter out noise and outliers. If this technique is efficient against salt and pepper noise, it has the reverse side of smoothing sharp edges.

Pan et al. (2019) considered closed boundaries and filled them using region growing. The selected pixels are then used to retrieve the corresponding 3D points. A refinement is operated using the optimal Otsu threshold, and the SOR algorithm. These operations allow to remove outlier points after the raster to points conversion.

On top of these first presented operations, very common tool are mathematical morphology operations.

Jung et al. (2019) perform different processes depending on the orientation of the markings, longitudinal or transversal. In both cases, an opening operation (erosion followed by dilation) is performed with a linear Structuring Element (SE). Its orientation depends on the orientation of the marking. For the erosion step, the authors recommend a structured element's length greater than the lane's width, in order to remove small False Positives (FP). They suggest also to use a bigger SE for the dilation to connect over-segmented parts.

Guan et al. (2014) perform a dilation to merge close connected components with a linear structuring element. The SE is oriented using the heading value of the sensor along the trajectory and with a length defined empirically. By doing so, this technique clearly favors longitudinal markings. Using the same procedure, Kumar et al. (2014) add a connected component filtering between the dilation and the erosion operations. The filtering uses CC shapes with prior knowledge about the road markings.

Guo et al. (2015) and Wan et al. (2019) proposed a closing procedure (dilation followed by erosion) to merge the elements close to each other.

It can be noticed that there is a tendency to use specific or adaptative SE (dimensions and orientation) for improving the results. Dilation and erosion operations are often jointly used, but the order in which they are applied can be different according to the authors. The paradigm depends on the strictness or sensitivity of the thresholding previously performed. Supposing a permissive threshold, the tendency will be to delete noise and so to perform an opening operation (so to begin with erosion). On the contrary, if the thresholding method is "stricter", shape reconstruction is a priority, so the first operation should be a dilation (closing procedure).

As introduced before, those operations try to reduce the noise on the thresholding results and to restore the shape of the markings. They can indirectly favor some types of markings and introduce prior knowledge. The main goal is also to reduce the over-segmentation of the objects that can be caused by occlusions or point density variations. Considering the current data as cleaned, the classification of the objects can be realized.

2.5 Classification and shape recognition

Different classification methods have been proposed in the literature in order to recognize and classify the markings. Road markings are of different types. The most obvious category is composed of linear elements, i.e. continuous or discontinuous lines such as traffic lane lines, stop lines, pedestrian crossings. Zebra lines are a bit apart due to their orientation, their non-rectangular shape and their possible combination with linear markings. Finally, the punctual markings, such as arrows, symbols, and texts composed the last category. All the presented papers do not manage all kind of markings. The approach depends on the used dataset. The classification step is very important as it assigns a meaning to the detected elements.

Before that, Cheng et al. (2017) and Yu et al. (2015) added an intermediary step consisting in decomposing potential markings clusters (sub-segmented elements).

Cheng et al. (2017) first try to decompose complex markings (e.g. clusters of zebras, sidelines connected with stop line...) into straight segments. The method is based on the detection of junction points. This is done by thresholding the neighborhood count of each pixel. The assumption is that a junction point has more neighbors than others. Then, handcrafted features are extracted for each connected component: area, perimeter, estimated width, orientation, and the Minimum Bounding Rectangle (MBR). A hierarchical tree coding *a priori* knowledge from the national standardization of road markings is then used to perform the classification.

Yu et al. (2015) also propose a method to decompose improperly connected markings. This special processing is applied to connected components having a bounding box diagonal length above a threshold. A voxel-based normalized cut segmentation (see Figure 2) is performed on these clusters of markings. After that, different processing steps are applied to the refined clusters. The large-size markings (centerline, boundary-line and stop line) are classified using their relative position and orientation with curb lines and the knowledge of the sensor's trajectory. The small markings (rectangles, pedestrian crossings, arrows, symbols...) are classified using a Deep Boltzmann Machine (DBM) able to extract complex features learned during a supervised training. Finally, the rest of the markings (zebra, dashed lines) are classified using a PCA to determine their orientation and then by studying their relative positions and orientation. The lane lines are thus reconstructed.

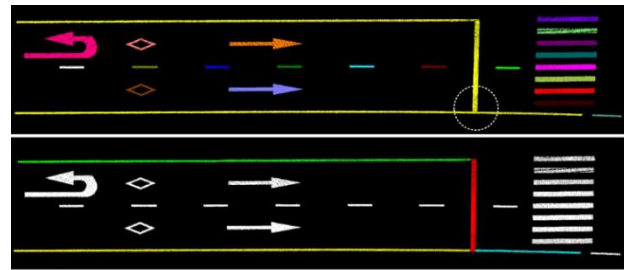


Figure 2. Voxel-based normalized cut segmentation (Yu et al., 2015).

Pan et al. (2019) use the bounding box information of each cluster to perform a first classification (length, diagonal angle, opposite size ratio). This basic classification allows to distinguish boundary lines, rectangles, and symbols. For the rest of the markings, the boundary of the cluster is estimated using the alpha-shape algorithm. A model matching procedure based on registration is then performed using Binary Shape Context (BSC) and Iterative Global Similarity Points (Pan et al., 2018).

Yao et al. (2018) also use the MBR for the classification of solid lines. For the rest of the markings, the deep learning network PointNet++ is used (Qi et al., 2017).

Guo et al. (2015) operate a Principal Component Analysis (PCA) on the connected component. The results allow to compute the principal direction of the cluster and to align it with the known template. The λ_1/λ_2 ratio (with λ_1 et λ_2 the two first eigen-values in descending order) allows to shorten the template candidates.

Soilán et al. (2017) begin the classification step by extracting handcrafted features describing the geometry of pixels' clusters: dimensions, area, bounding box, principal direction (using PCA), and pixel distribution along each principal direction. These features are put in a two-layer feedforward network that assigns markings into 3 classes: rectangles, arrows and others. For the first one, the orientation of the marking is compared with the trajectory. This allows to distinguish stop lines for instance. A neighborhood context analysis allows to classify pedestrian crossway (group of parallels markings with specific size and spacing). The procedure applied to classify arrows is similar to that of (Guo et al., 2015) : rotation of the data and then a model matching method is performed.

Fang et al. (2022) proposed to consider the adjacent markings during the classification. A subgraph describes the spatial relationship between the considered marking and its neighbors. The road marking problem is thus a node classification solved by a Graph Neural Network (GNN) model with multi-head attention mechanism.

Whatever handcrafted or learn features, fixed thresholds, decision trees or neural networks for the classification part, the proposed classification techniques are various, because it is a relatively difficult task. The more numerous markings type to classify, the finer the feature must be extracted. Considering the over-segmentation phenomenon, the potential misclassification also increases with the number of categories.

2.6 Deep-Learning approaches

This section is dedicated to paper that used deep learning approaches. They couldn't really be presented in the previous sections because they are not structured in the same way.

Mi et al. (2021) proposed a two-steps top-down approach. In the first step, YOLOv3 (Redmon and Farhadi, 2018) is used to predict positions, bounding boxes and labels from a feature map. In a second step, an energy function is optimized. It allows to finely position the marking shape inside the bounding box. A reranking procedure allows to handle misclassification during the first step.

Ma et al. (2021) introduced two capsule-based network architectures for road marking extraction and classification. The use of a capsule structure allows to extract high-level features.

Wen et al. (2019) proposed neural networks for the extraction and classification of the road markings. A modified U-net (Ronneberger et al., 2015) is used for the extraction. A multi-scale clustering allows the classification of large size marking while a Convolutional Neural Network (CNN) is used for smaller markings.

The image Deep-Learning approach suffers from a loss of information. Indeed, such neural networks have a fixed size of input. It induces that each marking must be represented on fixed size image, for instance on a 512x512 image. The input CC should be scaled, or a sliding windows approach should be used to overcome that.

2.7 Shape reconstruction and vectorization

After the classification, some over-segmented segments can remain, and merging operations might be required. To further reduce the over-segmentation, Jung et al. (2019) presented geometrics rules for segments merging. After a skeletonization of the remaining connected components, each of them can be considered as a segment. The polar line parametrization is used to describe the position and orientation of the segment. Different rules, defined as angle or distance threshold allow to do or do not merge two segments.

Barçon and Picard (2021), Jung et al. (2019), Yao et al (2021) proposed similar geometric considerations to perform a lane-line reconstruction from individual dash-lines. Taking a first marking, an azimuth search direction is defined. This marking is associated with neighbors under different constraints, i.e. having the same orientation, a similar shape, a distance between them and angle between the linking angle and a search direction below a threshold (see Figure 3). The procedure is repeated until there is no remaining element.

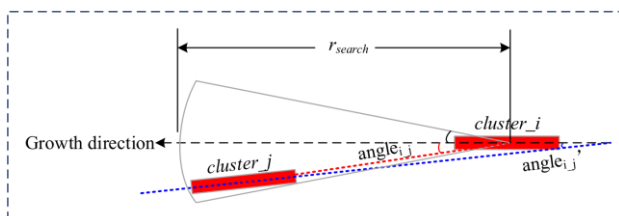


Figure 3. Lane line reconstruction procedure (Yao et al., 2018).

Pan et al. (2019) realize a polyline vectorization of the detected markings. For linear shaped objects, the points are adaptively sampled proportionally to the local curvature. For the rest of the markings that have been classified using model matching, the resulting position and orientation are used to generate a closed polyline at the right place. This allows to get rid of potential shape anomalies before the export.

Wan et al. (2019) proposed to cluster lane lines using their relative position with the trajectory in the transversal direction. It simplifies the problem in only one dimension for each linear position along the trajectory and allow to easily manage curves.

This type of post-processing can enhance the performance of the global process in case of occlusions. In fact, it is like an interpolation of the results where the data is missing. In order to constrain the interpolation process, some prior knowledge about the normalized shape of the markings is introduced.

3. WEAKNESSES

After this literature review, it is appropriate to summarize the different weaknesses encountered.

3.1 The input data

MLS point clouds are defined as an inhomogeneous and unordered data. As already discussed, dense point clouds are computationally hard to manipulate as they constitute heavy files. Their unstructured nature makes direct spatial analysis difficult or even impossible. The acquisition process generates inhomogeneous point density, causing a spatial over-sampling (useless information) and sub-sampling up to a total lack of information in some areas.

As mentioned before, overcoming the intensity inhomogeneity also constitutes a challenging task to distinguish road markings from the surrounding asphalt.

3.2 Non-conform geometry

Because of the demanding input data, some markings have not the expected conform geometry. The typical case is a long marking, incompletely extracted, whatever the reason is and consequently decomposed in smaller elements. These elements are of course misclassified, as they can match with others marking classes. The only way to avoid this behaviour of the algorithm, is to introduce further context information. And in a top-down approach, merge small element that belong to the same original marking. Wen et al. (2019) introduced some prior knowledge based on context. The assumption they made is that lane lines on both side of the road are continuous. The corresponding marking can thus be (re)connected. The authors also trained and used a cGAN (conditional Generative Adversarial Network) to automatically complete arrows and small markings shapes.

3.3 A comfortable general case

A lot of paper considers the general case, defined by a road well delimited by curbs. For many of them, the road point segmentation entirely depends on it. The segmentation is usually performed by the detection of abrupt altitude (or slope) variations. Anyway, they assume that two hypotheses are fulfilled.

Paper	Road or ground extraction	Intensity thresholding method	Shape improvement and filtering	Classification
(Cheng <i>et al.</i> , 2017)	Voxel upward growing region thresholding	Adaptative threshold based on scan-angle and range	Median filter and a minimum area threshold	Decision tree
(Fang <i>et al.</i> , 2022)	Cloth Simulation Filter (CSF)	Same as (Guan <i>et al.</i> , 2014)	Voxel-based Normalized cut	Graph Neural Network (GNN)
(Guan <i>et al.</i> , 2014)	Scan-line slope/altitude thresholding	Adaptative threshold depending on point density	Opening operation	#
(Guo, Tsai and Han, 2015)	Road altitude deducted from trajectory, cartesian plane fitting	Otsu threshold	Closing operation	PCA, handcrafted features and model matching
(Jaakkola <i>et al.</i> , 2008)	#	Intensity correction and simple thresholding	Opening then closing	Handcrafted features
(Jung <i>et al.</i> , 2019)	RANSAC 2nd order polynomial fitting	Expectation-Maximization	Opening operation	#
(Kumar <i>et al.</i> , 2013) & (Kumar <i>et al.</i> , 2014)	Image based: snake curve	Adaptative threshold using range	Opening operation	#
(Pan <i>et al.</i> , 2019)	Pseudo scan-line slope/ altitude thresholding	Maximum entropy optimal threshold	Region growing, Otsu, Statistical Outlier Removal (SOR)	Handcrafted features, alpha-shape, model matching
(Soilán <i>et al.</i> , 2017)	Voxel-based using trajectory	Adaptative Otsu threshold using scan-angle	Area and width/length ratio threshold	Handcrafted features, NN, trajectory, model matching
(Yang <i>et al.</i> , 2020)	Road altitude deducted from trajectory; transversal elevation thresholding	Thresholding profile by profile	Euclidian distance clustering between successive profiles	#
(Yao <i>et al.</i> , 2018)	Scan-line slope/ altitude thresholding	Adaptative threshold (Bradley and Roth, 2007)	Minimum connectivity threshold	Handcrafted features and PointNet++
(Ye <i>et al.</i> , 2020)	Voxel upward growing region thresholding	Double threshold using both intensity and distance to curb	Statistical Outlier Removal (SOR)	#
(Yu <i>et al.</i> , 2015)	Pseudo scan-line slope/ altitude thresholding	Adaptative Otsu threshold using range	Spatial density filtering	#
(Wan <i>et al.</i> , 2019)	Road altitude deducted from trajectory; transversal elevation thresholding	Iterative maximum entropy and median filtering	Closing operation	Handcrafted features
(Wen <i>et al.</i> , 2019)	Road boundary detection (Zai <i>et al.</i> , 2018)	Modified U-Net	#	Multiscale clustering/ CNN

Table 1. Summary of the state of the art

The first one is the existence of a curb, or at least a significant jump. And the second is that no other object can cause an abrupt altitude variation. However cars (parked or driving), pedestrians, and so on, can be scanned during a mobile mapping acquisition. In other words, this technique assumes that the scanned scene is an urbanized area composed of curbs and requires a very clean point cloud. Even under these conditions, common situations such as ramp curbs or crossway cause local failures...

It can also be noticed the use of the trajectory. Different processing chain assumed that the trajectory information is available. However, this information cannot always be obtained automatically. If the acquisition trajectory leads to multiple passing in the same street, eventually in the opposite directions, the raw trajectory cannot be used. The dependency on the trajectory can also mean that the proposed method cannot be applied on lane or areas where the sensor precisely doesn't cross.

4. CHALLENGES AND PERSPECTIVES

As presented previously, road markings detection, and at a greater scale point clouds understanding, is a very challenging issue. The perfect algorithm should be able to deal with missing and incomplete data. To do that, the algorithm should have a strong prior knowledge of what is expected. However, road scenes can be very varied. Some context information should be determined to trigger the use of prior knowledge. For road markings, an useful context information can be the position of road edges. Yu *et al.* (2015) exploit the results of the curb detection to enhance the classification of road markings.

It is also interesting to consider *a priori* knowledge on the markings themselves. First, the shape of each marking should follow a standardization defined by the competent authority. So, the shapes of individual markings are known in advance. A second research issue, less easy to encode and to implement, is the dependency between them. For instance, since the spacing of lines composing a pedestrian crossing is regular, this knowledge should allow to detect that one of its elements is missing.

However, encoding prior knowledge is not always that simple. Moreover, in complex scenes, with a lot of missing information, context deductions cannot really be applied as it would be considered as extrapolation. Road markings that do not severely follow the standardization can also be encountered, as observed in recent datasets.

Considering the limitations of the input data and the different innovative ways to threshold the intensity of points clouds, we consider that the principal room for improvement is now in the classification stage. The literature presents many features extraction methods and classifiers, leading to very good results. To go further, the classifier should consider more contextual information about the surrounding markings. It can also extract information from other objects detected in the scene (roads signs for instance) and confront them to prior knowledge. The improvement needed, can also maybe comes from exogeneous data. Barçon *et al.* (2022) used national vector road database as prior knowledge for road orientation for instance.

The Deep-Learning constitutes an exciting potential for top-down approaches. The principal inconvenient is the need of labelled data for the training. These approaches also do not allow to use the strong prior knowledge available on road markings

directly, a post-processing must be implemented. Nevertheless and as presented by (Fang *et al.*, 2022), neural networks can deal with more context information. The challenging task of manually encoding spatial relationships between road features might be directly and automatically learned by the network supposing that the training data are sufficient.

5. CONCLUSION

Road marking detection from dense MLS point cloud is a widely studied matter by the research community because of its miscellaneous potential applications. This paper presented a review of the different processing chains proposed over 10 years of the literature and highlighted their contribution. The different weaknesses of the proposed algorithm are summarized, and some perspectives have been given. The imperfect nature of the input data imposes very robust processing chains. Potentials improvement of the presented workflows could be found in the standardized shape of road markings, their relationship with others road furniture or exogeneous data i.e. by introducing prior knowledge.

6. REFERENCES

- Barçon, E., Landes, T., Grussenmeyer, P., Berson, G., 2022. Vectorization of Urban MLS Point Clouds: A Sequential Approach Using Cross Sections. *Int. Arch. Photogramm. Remote Sens. Spat. Inf. Sci.* XLIII-B2-2, 351–358. <https://doi.org/10.5194/isprs-archives-XLIII-B2-2022-351-2022>
- Barçon, E., Picard, A., 2021. Automatic detection and vectorization of linear and point objects in 3D point cloud and panoramic images from mobile mapping system. *Int. Arch. Photogramm. Remote Sens. Spat. Inf. Sci. - ISPRS Arch.* 43, 305–312. <https://doi.org/10.5194/isprs-archives-XLIII-B2-2021-305-2021>
- Bradley, D., Roth, G., 2007. Adaptive Thresholding using the Integral Image. *J. Graph. Tools* 12, 13–21. <https://doi.org/10.1080/2151237x.2007.10129236>
- Cheng, M., Zhang, H., Wang, C., Li, J., 2017. Extraction and Classification of Road Markings Using Mobile Laser Scanning Point Clouds. *IEEE J. Sel. Top. Appl. Earth Obs. Remote Sens.* 10, 1182–1196. <https://doi.org/10.1109/JSTARS.2016.2606507>
- Fang, L., Sun, T., Wang, S., Fan, H., Li, J., 2022. A graph attention network for road marking classification from mobile LiDAR point clouds. *Int. J. Appl. Earth Obs. Geoinf.* 108, 102735. <https://doi.org/10.1016/j.jag.2022.102735>
- Guan, H., Li, J., Yu, Y., Wang, C., Chapman, M., Yang, B., 2014. Using mobile laser scanning data for automated extraction of road markings. *ISPRS J. Photogramm. Remote Sens.* 87, 93–107. <https://doi.org/10.1016/j.isprsjprs.2013.11.005>
- Guo, J., Tsai, M.J., Han, J.Y., 2015. Automatic reconstruction of road surface features by using terrestrial mobile lidar. *Autom. Constr.* 58, 165–175. <https://doi.org/10.1016/j.autcon.2015.07.017>
- Jaakkola, A., Hyypä, J., Hyypä, H., Kukko, A., 2008. Retrieval algorithms for road surface modelling using laser- based

- mobile mapping. *Sensors* 8, 5238–5249. <https://doi.org/10.3390/s8095238>
- Jung, J., Che, E., Olsen, M.J., Parrish, C., 2019. Efficient and robust lane marking extraction from mobile lidar point clouds. *ISPRS J. Photogramm. Remote Sens.* 147, 1–18. <https://doi.org/10.1016/j.isprsjsprs.2018.11.012>
- Kumar, P., McElhinney, C.P., Lewis, P., McCarthy, T., 2014. Automated road markings extraction from mobile laser scanning data. *Int. J. Appl. Earth Obs. Geoinf.* 32, 125–137. <https://doi.org/10.1016/j.jag.2014.03.023>
- Kumar, P., McElhinney, C.P., Lewis, P., McCarthy, T., 2013. An automated algorithm for extracting road edges from terrestrial mobile LiDAR data. *ISPRS J. Photogramm. Remote Sens.* 85, 44–55. <https://doi.org/10.1016/j.isprsjsprs.2013.08.003>
- Ma, L., Li, Y., Li, J., Yu, Y., Junior, J.M., Goncalves, W.N., Chapman, M.A., 2021. Capsule-Based Networks for Road Marking Extraction and Classification from Mobile LiDAR Point Clouds. *IEEE Trans. Intell. Transp. Syst.* 22, 1981–1995. <https://doi.org/10.1109/TITS.2020.2990120>
- Mi, X., Yang, B., Dong, Z., Liu, C., Zong, Z., Yuan, Z., 2021. A two-stage approach for road marking extraction and modeling using MLS point clouds. *ISPRS J. Photogramm. Remote Sens.* 180, 255–268. <https://doi.org/10.1016/j.isprsjsprs.2021.07.012>
- Otsu, N., 1979. A Threshold Selection Method from Gray-Level Histograms. *IEEE Trans. Syst. Man Cybern.* 9, 62–66. <https://doi.org/10.1109/TSMC.1979.4310076>
- Pan, Y., Yang, B., Li, S., Yang, H., Dong, Z., Yang, X., 2019. Automatic road markings extraction, classification and vectorization from mobile laser scanning data, in: *International Archives of the Photogrammetry, Remote Sensing and Spatial Information Sciences - ISPRS Archives*. pp. 1089–1096. <https://doi.org/10.5194/isprs-archives-XLII-2-W13-1089-2019>
- Pan, Y., Yang, B., Liang, F., Dong, Z., 2018. Iterative global similarity points: A robust coarse-to-fine integration solution for pairwise 3D point cloud registration. *Proc. - 2018 Int. Conf. 3D Vision, 3DV 2018* 180–189. <https://doi.org/10.1109/3DV.2018.00030>
- Qi, C.R., Yi, L., Su, H., Guibas, L.J., 2017. PointNet++: Deep hierarchical feature learning on point sets in a metric space. *Adv. Neural Inf. Process. Syst.* 2017-December, 5100–5109.
- Redmon, J., Farhadi, A., 2018. YOLOv3: An Incremental Improvement. <https://doi.org/10.48550/arXiv.1804.02767>
- Ronneberger, O., Fischer, P., Brox, T., 2015. U-Net: Convolutional Networks for Biomedical Image Segmentation, in: *International Conference on Medical Image Computing and Computer-Assisted Intervention*. Springer International Publishing, pp. 234–241. https://doi.org/10.1007/978-3-319-24574-4_28
- Soilán, M., Riveiro, B., Martínez-Sánchez, J., Arias, P., 2017. Segmentation and classification of road markings using MLS data. *ISPRS J. Photogramm. Remote Sens.* 123, 94–103. <https://doi.org/10.1016/j.isprsjsprs.2016.11.011>
- Wan, R., Huang, Y., Xie, R., Ma, P., 2019. Combined Lane Mapping Using a Mobile Mapping System. *Remote Sens.* 11, 305. <https://doi.org/10.3390/rs11030305>
- Wen, C., Sun, X., Li, J., Wang, C., Guo, Y., Habib, A., 2019. A deep learning framework for road marking extraction, classification and completion from mobile laser scanning point clouds. *ISPRS J. Photogramm. Remote Sens.* 147, 178–192. <https://doi.org/10.1016/j.isprsjsprs.2018.10.007>
- Yang, R., Li, Q., Tan, J., Li, S., Chen, X., 2020. Accurate Road Marking Detection from Noisy Point Clouds Acquired by Low-Cost Mobile LiDAR Systems. *ISPRS Int. J. Geo-Information* 9, 608. <https://doi.org/10.3390/ijgi9100608>
- Yao, L., Chen, Q., Qin, C., Wu, H., Zhang, S., 2018. Automatic Extraction Of Road Markings From Mobile Laser-Point Cloud Using Intensity Data. *Int. Arch. Photogramm. Remote Sens. Spat. Inf. Sci.* XLII-3, 2113–2119. <https://doi.org/10.5194/isprs-archives-XLII-3-2113-2018>
- Yao, L., Qin, C., Chen, Q., Wu, H., 2021. Automatic road marking extraction and vectorization from vehicle-borne laser scanning data. *Remote Sens.* 13. <https://doi.org/10.3390/rs13132612>
- Ye, C., Zhao, H., Ma, L., Jiang, H., Li, H., Wang, R., Chapman, M.A., Junior, J.M., Li, J., 2020. Robust Lane Extraction From MLS Point Clouds Towards HD Maps Especially in Curve Road. *IEEE Trans. Intell. Transp. Syst.* 1–14. <https://doi.org/10.1109/TITS.2020.3028033>
- Yu, Y., Li, J., Guan, H., Jia, F., Wang, C., 2015. Learning hierarchical features for automated extraction of road markings from 3-D mobile LiDAR point clouds. *IEEE J. Sel. Top. Appl. Earth Obs. Remote Sens.* 8, 709–726. <https://doi.org/10.1109/JSTARS.2014.2347276>
- Zai, D., Li, J., Guo, Y., Cheng, M., Lin, Y., Luo, H., Wang, C., 2018. 3-D Road Boundary Extraction from Mobile Laser Scanning Data via Supervoxels and Graph Cuts. *IEEE Trans. Intell. Transp. Syst.* 19, 802–813. <https://doi.org/10.1109/TITS.2017.2701403>
- Zhang, H., Li, J., Cheng, M., Wang, C., 2016. Rapid Inspection of Pavement Markings Using Mobile Lidar Point Clouds. *ISPRS - Int. Arch. Photogramm. Remote Sens. Spat. Inf. Sci.* XLI-B1, 717–723. <https://doi.org/10.5194/isprsarchives-XLI-B1-717-2016>
- Zhang, W., Qi, J., Wan, P., Wang, H., Xie, D., Wang, X., Yan, G., 2016. An easy-to-use airborne LiDAR data filtering method based on cloth simulation. *Remote Sens.* 8, 501. <https://doi.org/10.3390/rs8060501>